

Topological superconducting phase and Majorana bound states in Shiba chains

This content has been downloaded from IOPscience. Please scroll down to see the full text.

2015 Phys. Scr. 2015 014008

(<http://iopscience.iop.org/1402-4896/2015/T164/014008>)

View [the table of contents for this issue](#), or go to the [journal homepage](#) for more

Download details:

IP Address: 78.53.41.164

This content was downloaded on 02/09/2015 at 19:41

Please note that [terms and conditions apply](#).

Topological superconducting phase and Majorana bound states in Shiba chains

Falko Pientka¹, Yang Peng¹, Leonid Glazman² and Felix von Oppen¹

¹Dahlem Center for Complex Quantum Systems and Fachbereich Physik, Freie Universität Berlin, D-14195 Berlin, Germany

²Department of Physics, Yale University, New Haven, CT 06520, USA

E-mail: vonoppen@physik.fu-berlin.de

Received 13 October 2014

Accepted for publication 8 May 2015

Published 25 August 2015



Abstract

Chains of magnetic adatoms on a conventional superconducting substrate constitute a promising venue for realizing topological superconductivity and Majorana end states. Here, we give a brief overview over recent attempts to describe these systems theoretically, emphasizing how the topological phase emerges from the physics of individual magnetic impurities and their associated Shiba states.

Keywords: topological superconductivity, Majorana fermions, magnetic adatoms

(Some figures may appear in colour only in the online journal)

1. Introduction

Perhaps the most promising route towards realizing Majorana states in condensed matter systems relies on helical electron systems in one dimension (1D), proximity coupled to a conventional s -wave superconductor [1, 2]. This possibility was first suggested for topological insulators by Fu and Kane [3, 4] and subsequently extended to a number of other platforms such as semiconductor quantum wires [5–7]. There has been considerable progress towards implementing these platforms experimentally, including possible evidence for Majorana bound states in semiconductor quantum wires [8–15].

These platforms realize a topological superconducting phase which is adiabatically connected to a spinless p -wave superconductor in 1D [16, 17]. This is achieved by three essential ingredients, proximity coupling of the 1D system to a conventional s -wave superconductor, a Zeeman field, and spin–orbit coupling. This can be roughly understood as follows: inducing superconductivity by proximity ensures that the superconducting correlations are inherited from a bulk system and hence not subject to the Mermin–Wagner theorem despite their 1D nature. The Zeeman field spin polarizes the electrons, making the system akin to spinless fermions. Rashba spin–orbit coupling is needed to enable proximity coupling of a conventional s -wave superconductor to a spin-polarized system in which superconducting order must

(typically) be of p -wave nature. Note that the spin–orbit coupling can be located either in the 1D system [4–6] or in the bulk superconductor [18, 19].

Here, we discuss an alternative platform that also relies on these general ideas, namely a chain of magnetic adatoms placed on a superconductor. This platform was recently suggested in [20], building on previous related works [21–23]. We focus on an analytical approach which describes the physics of the adatom chain and its topological phases starting with the physics of an individual magnetic adatom [24–26].

Recently, a first experiment which may have realized a version of this scenario has appeared in the literature [27]. In this experiment, a chain of Fe adatoms is placed on a superconducting Pb (110) surface. Evidence for Majorana end states is provided by scanning tunneling microscopy measurements which can resolve possible end states both in real space and in energy.

2. Shiba states

2.1. Individual magnetic impurity

We start by considering the physics of a single magnetic impurity in a conventional superconductor. This is a classic problem in the theory of superconductors [28–31]. For simplicity, let us assume that the adatom is electronically inert

and interacts with the electrons in the superconductor only by exchange coupling with its spin S . If the spin is sufficiently large, we can assume it to be classical. The effect of a single magnetic impurity on the superconductor can be readily analyzed by means of the Bogoliubov–deGennes (BdG) Hamiltonian (see, e.g., [24] for a more detailed account)

$$H = \left(\frac{p^2}{2m} - \mu \right) \tau_z + JS \cdot \sigma \delta(\mathbf{r}) + \Delta_0 \tau_x. \quad (1)$$

Here, J denotes the strength of the exchange coupling between impurity spin (located at the origin) and electron spins in the superconductor, Δ_0 the pairing strength of the superconductor, and σ_j (τ_j) denotes Pauli matrices in spin (particle–hole) space. It was already shown in the 60s that this Hamiltonian has a subgap bound state localized at the impurity spin, often referred to as Yu–Shiba–Rusinov state [28–30]—or simply Shiba state for brevity. Its energy is

$$E_0 = \Delta_0 \frac{1 - \alpha^2}{1 + \alpha^2}, \quad (2)$$

where $\alpha = \pi \nu_0 S J$ is a dimensionless measure of the strength of the exchange coupling with ν_0 the normal-state density of states of the superconductor. Note that the Shiba energy can change sign when $\alpha = 1$. This point signals a quantum phase transition where the impurity effectively binds an electron and the many-body ground state of the superconductor changes from even to odd electron number parity.

For our purposes, Shiba bound states have two essential properties which are encoded in their BdG wavefunctions

$$\begin{aligned} u_\uparrow(\mathbf{r}) &\sim \frac{\sin(k_F r - \delta)}{k_F r} e^{-r/\xi_E}, \\ v_\downarrow(\mathbf{r}) &\sim \frac{\sin(k_F r + \delta)}{k_F r} e^{-r/\xi_E}, \\ u_\downarrow(\mathbf{r}) &= v_\uparrow(\mathbf{r}) = 0, \end{aligned} \quad (3)$$

where δ is a phase shift which depends on the strength of the exchange coupling, $\tan \delta = -1/\alpha$. First, the Shiba states are linear combinations of spin-up electrons and spin-down holes and are thus perfectly *spin polarized* along the direction of the classical impurity spin \mathbf{S} . Second, their wave function initially decays as $1/r$ away from the impurity which crosses over into an exponential decay only for distances larger than

$$\xi_E = \frac{\hbar v_F}{\sqrt{\Delta_0^2 - E_0^2}}. \quad (4)$$

Specifically, for deep Shiba states with energy $E_0 \ll \Delta_0$, this exponential decay becomes relevant only on the scale of the superconducting coherence length $\xi_0 = \hbar v_F / \Delta_0$.

2.2. Chain of magnetic impurities

An individual magnetic impurity provides a Shiba state within the superconducting gap while the impurity d -levels are far from the Fermi energy of the superconductor and thus electronically inert beyond the formation of the local moment. Now, consider a chain of magnetic impurities. If the adatoms

are sufficiently dilute, direct hopping between the adatom d -levels is weak and the resulting band of adatom d -levels remains electronically inert. In this limit, each magnetic impurity contributes a Shiba state. These Shiba states hybridize and broaden out into a Shiba band. Below, we refer to this situation as Shiba chain and analyze it in detail in section 3. This section reviews work in [24, 25].

A different picture emerges when the adatoms are closely spaced and the direct hopping between the adatom d -levels becomes significant. In this case, the width of the adatom d -band can become so large that it crosses the Fermi energy of the substrate superconductor. In this case, the adatom d -levels are no longer electronically inert but have to be included in a low-energy description. Effectively, the adatom d -levels form a 1D wire so that we refer to this situation below as wire limit. This situation will be discussed in section 4 which reviews work in [26].

3. Shiba chains

3.1. Simple model

When the adatom d -levels remain electronically inert, we can focus attention on the Shiba states induced in the gap of the superconducting substrate. If the Shiba states are sufficiently deep and the broadening sufficiently small, we can focus attention on the Shiba states only and project out the quasi-particle continua at higher energies [24]. Then, we can write an effective low-energy Hamiltonian in terms of the creation operator c_j^\dagger associated with the Shiba state at site j . Neighboring Shiba states hybridize with amplitude t (see below for a more careful discussion). In this limit, it is tempting to describe the Shiba chain by a Hamiltonian of the form

$$\begin{aligned} \mathcal{H} = E_0 \sum_j c_j^\dagger c_j - t \sum_j [c_{j+1}^\dagger c_j + c_j^\dagger c_{j+1}] \\ + \Delta \sum_j [c_{j+1} c_j + c_j^\dagger c_{j+1}^\dagger]. \end{aligned} \quad (5)$$

As the Shiba chain is embedded into the host superconductor, we include a pairing term of strength Δ into this Hamiltonian. Importantly, the pairing term necessarily involves pairing correlations between different sites due to the perfect spin polarization.

While this Hamiltonian neglects essential physics of Shiba chains as discussed in section 3.3 below, it is a useful reference point due to its simplicity. In fact, equation (5) is just the Kitaev-chain Hamiltonian of a spinless p -wave superconductor, where the energy of the Shiba state plays the role of the chemical potential. (For the Shiba chain, the physical chemical potential is fixed to be in the center of the gap of the host superconductor and is set to zero for simplicity.) As is well-known, the Kitaev chain has a topological phase at finite Δ whenever the chemical potential is situated in the normal-state band, i.e., for $|E_0| < 2t$ in the present case. The corresponding phase diagram as a function of E_0 and Δ is shown in figure 1.

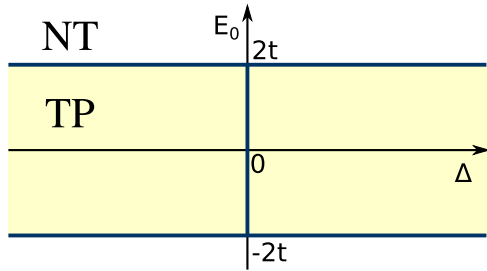


Figure 1. The phase diagram of the simplified Shiba-chain Hamiltonian (5) as function of p -wave pairing strength Δ and Shiba-state energy E_0 . This Hamiltonian is just the Hamiltonian of a Kitaev chain with the Shiba-state energy E_0 playing the role of the chemical potential. Thus, the Shiba-chain model has a topological superconducting phase (labeled by TP) as long as $|E_0| < 2t$, and a nontopological phase (labeled as NT) otherwise. Note that this Hamiltonian neglects the power-law decay of the Shiba bound states which modifies the phase diagram as discussed below.

Thus, we find the following basic (though simplified—see section 3.3 below) picture for the phase diagram of Shiba chains [20, 24], see figure 2. When the magnetic adatoms are far apart, each of them is associated with a Shiba state and hybridization can be neglected. Clearly, in this case, the system is nontopological with $|E_0| > 2t$. As the adatoms are placed closer together, the hybridization increases and with it the bandwidth of the Shiba bands. Initially, the Shiba bands (including the BdG partner with an energy of opposite sign) still do not cross the chemical potential at the center of the gap. Thus, we still have $|E_0| > 2t$ and the system remains in the topologically trivial phase. Eventually, the two Shiba bands will extend beyond the center of the gap. Now, the pairing correlations Δ within the Shiba bands will again open a gap at the Fermi energy, but this is a p -wave gap, unlike the larger s -wave gap of the host superconductor! In this phase, the Shiba chain is in a topological phase and will host zero-energy Majorana bound states at its ends.

3.2. Induced pairing correlations

So far, we have simply assumed that the effective Kitaev-chain Hamiltonian for the Shiba chain contains pairing terms, but did not discuss their microscopic origin. This question is actually closely related to the collective behavior of the impurity spins. We noted that the Shiba states are spin polarized along the direction of the corresponding impurity spin, but ignored the question of how the impurity spins are oriented with respect to one another. This question is of obvious importance for the physics of the adatom chain. Indeed, we expect that the impurity spins interact through the familiar RKKY interaction mediated by the host superconductor and may thus order magnetically [32]. Two such orderings have been predominantly discussed in the literature [20, 24, 25, 33–35], which actually entail somewhat different physics of the pairing terms

One plausible possibility is that the chain orders ferromagnetically, with all impurity spins aligning along

a certain direction³. In that case, also all Shiba states along the chain are spin polarized along the same direction. This corresponds to a perfectly spin-polarized system and consequently, the spin-singlet Cooper pairs of a pure s -wave host superconductor would not be able to proximity-couple to the chain of Shiba states. To induce pairing correlation within the chain of Shiba states in this case, we need to rely on (Rashba) spin-orbit coupling in the superconducting substrate.

An interesting alternative is that the magnetic impurities form a spin helix in which the impurity spins rotate along the chain [20, 24, 25, 33–35]. In this case, neighboring impurity spins are not aligned and the corresponding Shiba states are polarized along different directions. The spin singlet Cooper pairs of the host superconductor can effectively proximity-couple to the chain as long as the spin-up electron and the spin-down electron enter on different sites. Thus, the effective pairing correlations which result from these processes are just of the spinless p -wave type which are included in the Kitaev-chain Hamiltonian (5).

These considerations suggest that that Rashba spin-orbit coupling and helical spin ordering are closely related. This can indeed be shown explicitly for the Hamiltonian of a 1D semiconductor quantum wire with spin-orbit coupling of strength α and subject to a Zeeman field \mathbf{B} [22, 37],

$$H = \frac{1}{2m}(p + m\alpha\sigma_z)^2 - \mathbf{B} \cdot \boldsymbol{\sigma}. \quad (6)$$

The canonical transformation $U = \exp(imax\sigma_z)$, where x denotes the coordinate along the wire, yields

$$H \rightarrow H' = \frac{p^2}{2m} - \mathbf{B}(x) \cdot \boldsymbol{\sigma}. \quad (7)$$

Here $\mathbf{B}(x)$ is a helical Zeeman field which rotates along the chain about the z -direction with wavevector $2m\alpha$. This establishes an exact mapping between Rashba spin-orbit coupling and a helical order of the adatom spins.

A similar unitary transformation can also be applied to the helical Shiba chain. Consider the corresponding Hamiltonian

$$H = \left(\frac{p^2}{2m} - \mu \right) \tau_z + J \sum_j \mathbf{S}_j \cdot \sigma \delta(\mathbf{r} - \mathbf{R}_j) + \Delta_0 \tau_x, \quad (8)$$

where $\mathbf{R}_j = ja\hat{\mathbf{x}}$ denotes the positions of the magnetic adatoms and \mathbf{S}_j denotes a spin helix

$$\mathbf{S}_j = (\sin \theta \cos \phi_j, \sin \theta \sin \phi_j, \cos \theta). \quad (9)$$

The spin helix advances along the chain as $\phi_j = k_h ja$ with opening angle θ with respect to the z -axis. We can now perform the unitary transformation $U = \exp(ik_h x \sigma_z / 2)$. This rotates all spins such that the exchange coupling of the electron spins involves the same impurity spin direction $\mathbf{S} = (\sin \theta, 0, \cos \theta)$ for all sites. At the same time, it introduces a spin-orbit-coupling-like term into the kinetic

³ In the present context, this possibility was emphasized by Ali Yazdani at the Nobel Symposium *New Forms of Matter—Topological Insulators and Superconductors*; see also [36] for a subsequent calculation for a specific model of a two-dimensional superconductor.

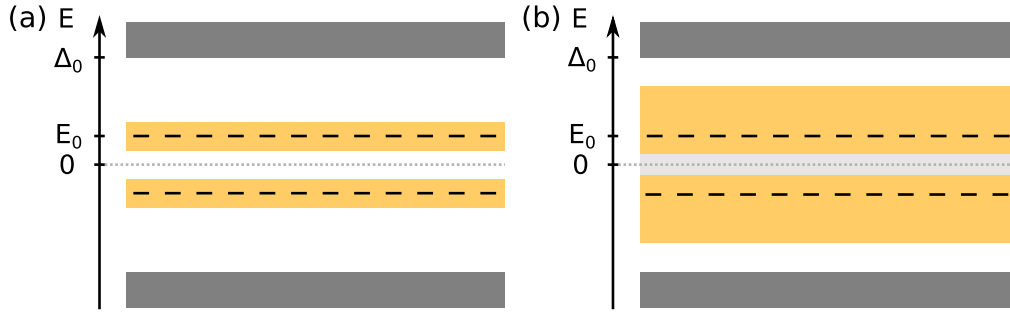


Figure 2. Excitation spectrum of Shiba chains as function of the distance between adatoms. (a) For dilute atoms, the Shiba states of the individual adatoms broaden out into bands, but these do not cross the chemical potential in the center of the gap. In this case, the system is in a nontopological phase. (b) For dense adatoms, the hybridization of the Shiba states becomes stronger and the Shiba band overlap at the center of the gap. In this case, the pairing correlations Δ reopen a gap which is of p -wave nature due to the spin polarization of the Shiba states. This is a topological superconducting phase which hosts Majorana bound states at its ends.

energy,

$$H = \left[\frac{(p_x + k_h \sigma_z / 2)^2 + p_\perp^2}{2m} - \mu \right] \tau_z + J \sum_j \mathbf{S} \cdot \sigma \delta(\mathbf{r} - \mathbf{R}_j) + \Delta_0 \tau_x. \quad (10)$$

We would like to make two comments on this transformed result: first, the spin-orbit field points along the z -direction while the adatoms induce an effective Zeeman field along a direction which is tilted by an angle θ away from the z -axis. It is well-known that the optimal situation for topological superconductivity requires orthogonal Zeeman and spin-orbit fields. In the present context, this is realized for a planar spin helix with $\theta = \pi/2$. Conical spin helices with smaller opening angles are less favorable. We find that this is indeed the case from more detailed calculations, as discussed below. Second, the effective spin-orbit coupling in equation (10) differs from Rashba spin-orbit coupling in that it affects only the p_x -term in the kinetic energy. With the surface of the superconductor is the xy -plane, conventional Rashba coupling would involve the combination $p_x \sigma_y - p_y \sigma_x$ ⁴. Apart from an inconsequential rotation in spin space, this differs from equation (10) in that it involves two Pauli matrices. However, the principal purpose of the spin-orbit coupling is to allow for p -wave superconducting correlations in the chain which derives from the term which involves the momentum *along* the chain. The term in the Rashba spin-orbit coupling involving the perpendicular direction modifies the physics merely quantitatively, but not qualitatively.

There is some experimental evidence for normal-metal substrates that chains of magnetic adatoms (Fe on Ir substrates) can indeed exhibit helical spin order [38]. More generally, spin helix formation is expected to occur when the adatom chain is embedded in a strictly 1D system [33–35]. In

this case, the RKKY interaction between the magnetic moments of the adatoms becomes maximal at $2k_F$. In the absence of fluctuations, this maximum at a finite wavevector induces spin-helix formation at wavevector $2k_F$. For not too strong thermal fluctuations, this order persists up to exponentially large lengths due to the linear dispersion of the spin-wave excitations of the spin helix [33]. These arguments depend only mildly on whether the substrate is normal or superconducting. The two cases differ only on length scales beyond the superconducting coherence length which is typically large compared to the pitch of the spin helix. For higher-dimensional substrates, the RKKY interaction typically favors ferromagnetic spin arrangements unless spin-orbit coupling induces a significant Dzyaloshinski–Moriya-type interaction between the adatom spins [39].

3.3. Kitaev chain with long-range hopping and pairing

3.3.1. Long-range hopping and pairing. So far, we have used that the Shiba states are spin polarized but ignored the fact that their wavefunctions initially decay as a power law away from the impurity. This is justified as long as the spacing between Shiba states is comparable to or larger than the coherence length of the host superconductor. However, typical experimental realizations will rather consist of chains where the magnetic adatoms are spaced on the scale of the lattice spacing of the host which is orders of magnitudes smaller than the coherence length. In this limit, we should take the power-law decay of the Shiba bound states into account. In fact, it is even conceivable that the entire length of the adatom chain remains smaller than or comparable to the coherence length so that it may be a good approximation to neglect the ultimate exponential decay of the Shiba states altogether.

Unlike the Kitaev-chain Hamiltonian with nearest-neighbor hopping and pairing, the effective low-energy Hamiltonian of Shiba chains with closely spaced adatoms should include longer-range hopping and pairing terms which result from the slow power-law decay of the Shiba states. Reflecting the decay of the Shiba wavefunctions, hopping and pairing decays with distance also as $1/r$. This power-law

⁴ Strictly speaking, the Rashba spin-orbit term would take a form similar to the transformed kinetic energy only for 2D superconductors. In 3D, the physical Rashba spin-orbit coupling would be limited to the surface of the superconductor. Again, this presumably affects the topological physics of the Shiba chain only quantitatively.

decay raises interesting questions which we want to address in the remainder of this section:

- It is well-known from the theory of phase transitions that long-range coupling can significantly modify the phase diagram of a model, especially in low dimensions. Thus, it is an interesting question to which degree the phase diagrams differ between the conventional Kitaev chain with nearest-neighbor hopping and pairing and the Kitaev chain with long-range coupling. We will focus on the case of a helical spin arrangement for which we can consider the phase diagram as function of the energy of the individual Shiba states (i.e., the strength of the exchange coupling between impurity and electron spins) and the helix wavevector (measured in units of the Fermi wavevector of the superconducting substrate). The results should also apply at least qualitatively to a ferromagnetic spin arrangement, with the helix wavevector being replaced by the strength of the Rashba spin-orbit coupling. One may also be interested to which degree the phase diagram differs for planar and conical spin helices.
- A hallmark of topological phases are exponentially localized end, edge, or surface states. Specifically, the Majorana bound states of 1D superconductors are localized exponentially near the end or at a domain wall. It seems likely that generically, power-law hopping and pairing is incompatible with such exponential localization. What then is the localization behavior of Majorana bound states and what is the nature of the topological phase transition? One may also question whether Hamiltonians with power-law couplings actually exhibit true topological phases.
- The last question can also be given a more experimental touch: are Majorana end states sufficiently localized in the presence of long-range coupling given the finite length of the chain? This is a relevant question because the chain length in experiment can be smaller than or comparable to the coherence length of the host superconductor [27]. Generically, the localization length of Majorana end states is governed by the topological gap which is smaller than the gap of the host superconductor. Thus, unless the relevant velocity is much smaller than the Fermi velocity of the superconductor (see section 4 below for a possible scenario in which this is actually the case), the Majorana end states in Shiba chains should be localized on scales larger than the coherence length ξ_0 of the host superconductor. This would imply that the Majorana end states strongly overlap, precluding experimental observation of reasonably separated Majorana excitations.

To address these questions, we have derived a tight-binding model starting from the Shiba states of the individual impurities [24, 25]. This model assumes that we are dealing with deep Shiba states with sufficiently weak hybridization such that we can project out the quasiparticle continuum of the host superconductor and focus on the Shiba states only.

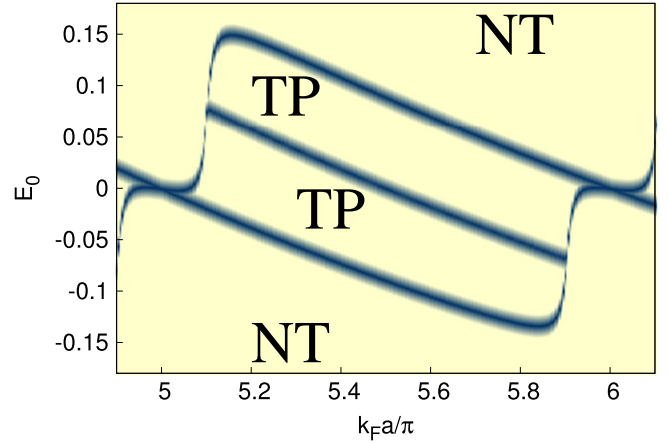


Figure 3. The phase diagram of a Shiba chain with planar spin helix when including the long-range hopping and pairing. The system exhibits topological (TP) and nontopological (NT) phases.

As shown in detail in [24], this leads to a Kitaev-like model,

$$\begin{aligned} \mathcal{H} = E_0 \sum_j c_j^\dagger c_j - \sum_{ij} t_{ij} [c_j^\dagger c_i + c_i^\dagger c_j] \\ + \sum_{ij} \Delta_{ij} [c_j c_i + c_i^\dagger c_j^\dagger]. \end{aligned} \quad (11)$$

For a planar spin helix of wavevector k_h , we find the long-range hopping amplitudes

$$t_{ij} = \Delta_0 \frac{\sin k_F r_{ij}}{k_F r_{ij}} e^{-r_{ij}/\xi_0} \cos k_h x_{ij}/2 \quad (12)$$

as well as the long-range pairing strengths

$$\Delta_{ij} = i\Delta_0 \frac{\cos k_F r_{ij}}{k_F r_{ij}} e^{-r_{ij}/\xi_0} \sin k_h x_{ij}/2 \quad (13)$$

for $i \neq j$. (Note that $t_{ii} = \Delta_{ii} = 0$.) Here, Δ_0 denotes the pairing strength of the host superconductor, k_F is its Fermi wavevector, $x_{ij} = (i - j)a$ in terms of the lattice spacing a of the chain, and $r_{ij} = |x_{ij}|$. Explicit results for conical spin helices can be found in [24].

3.3.2. Phase diagram. For an infinite chain, the tight-binding model can be diagonalized in momentum space. It is then straightforward to obtain the phase diagram of the model [24]. Focusing first on a planar spin helix of a certain helix wavevector, the resulting phase diagram as function of Shiba-state energy and Fermi wavevector of the superconducting substrate is shown in figure 3. The phase diagram exhibits both topological and nontopological regions. The outer tilted phase boundaries just reflect the fact that the model undergoes a transition from the topological to the nontopological phase as the (absolute value of the) energy of the Shiba state increases. Unlike the simplified model Hamiltonian (5) with nearest-neighbor hopping and pairing, these phase boundaries are tilted. This is a consequence of the long-range hopping which makes the Shiba bands depend on

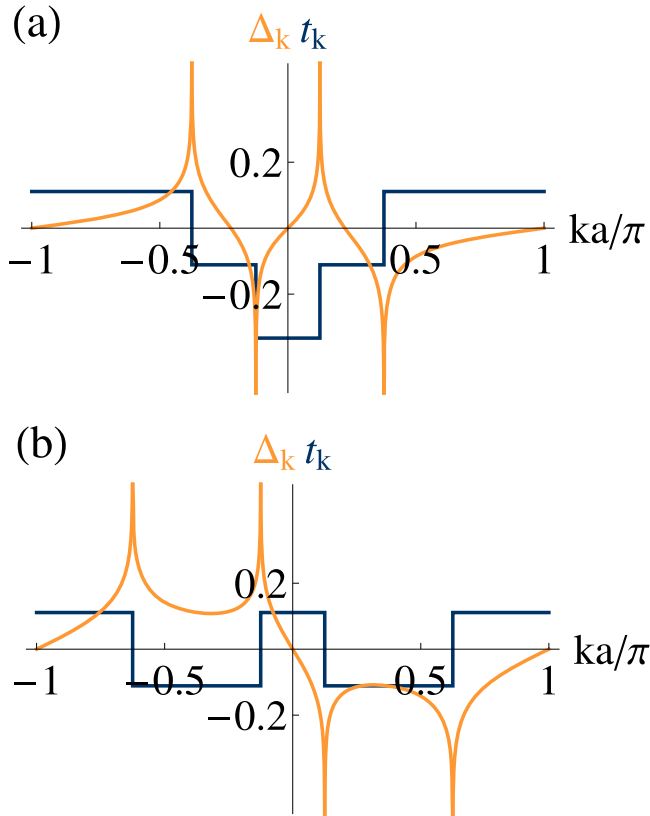


Figure 4. Normal-state dispersions t_k and gap function Δ_k for (a) *type-1* and (b) *type-2* dispersions of the Shiba-chain Hamiltonian (11).

the Fermi wavelength of the underlying superconducting substrate.

Apart from these conventional (albeit modified) phase boundaries, there are also phase boundaries that have no analog in the model (5) without long-range coupling. First, there is an intermediate line in the middle between the outer two tilted phase boundaries. At this line, the gap merely collapses but the system remains topological on *both* sides. Second, there are nearly vertical phase boundaries which connect the upper and lower tilted phase boundaries.

To understand these new phase boundaries, we analyze the normal-state dispersion $t_k = \sum_j t_{ij} e^{ikx_{ij}}$ and the gap function $\Delta_k = \sum_j \Delta_{ij} e^{ikx_{ij}}$ more closely. These Fourier transforms can be readily performed explicitly [24]. For the realistic case of a coherence length which is large compared to the adatom spacing, the Fourier transform is dominated by the $1/r$ dependence of the hopping amplitudes and the pairing. Accordingly, one finds that t_k exhibits steplike behavior while Δ_k exhibits logarithmic singularities. The steps have a width of order $1/\xi_0$ and the bandwidth of the dispersion is of order $\Delta_0/k_F a$. Representative examples of these functions are shown in figure 4.

These Fourier transforms explain the origin of the additional phase boundaries. First consider the additional vertical phase boundaries in figure 3. These phase boundaries are associated with the fact that there are two distinct types of dispersions depending on the Fermi wavevector k_F and the

helix wavevector k_h —termed *type 1* and *type 2* in figure 4. The dispersion can have two or four Fermi points, with abrupt transitions between these two cases in the limit $\xi_0 \rightarrow \infty$. For two Fermi points, the Shiba chain has only a single right- and a single left-moving channel and pairing induces a true topological phase. In contrast, for four Fermi points, there are two left-moving and two right-moving Fermi points and the Shiba chain is effectively behaving like a two-channel wire. At each end, there are Majorana end states associated with both channels. These two Majorana end states hybridize and thus, the Shiba chain is in a nontopological phase. The nature of the dispersion depends on the relation between the Fermi wavevector k_F of the substrate and the helix wavevector k_h , and thus causes a vertical phase boundary in the phase diagram in figure 3.

The additional tilted line where the gap collapses in between two topological regions is a consequence of the horizontal section of the dispersion t_k . When the Fermi energy just coincides with this horizontal section, there is always one wavevector k on this horizontal section for which the gap function Δ_k vanishes, implying that the excitation gap collapses. This can be seen from the plot of Δ_k in figure 4.

We conclude this section by noting that the phase diagram changes qualitatively for a conical spin helix. Essentially, the conical spin helix breaks the symmetry of the dispersion under $k \rightarrow -k$. This suppresses the resonance underlying Cooper-pair formation and suppresses the topological superconducting phase, yielding a sizable gapless phase in the phase diagram. This case was analyzed more systematically in [24].

3.4. Majorana bound states

The vertical phase boundaries are actually rather unusual topological phase boundaries [25]: in the limit $\xi_0 \rightarrow \infty$, they constitute discontinuous topological phase transitions. Indeed, in this limit the gap does not close as one approaches the critical line from either side but rather discontinuously changes sign. This is associated with the fact that the dispersion jumps discontinuously between *type 1* and *type 2* at the transition. For a finite but large ξ_0 , the transition becomes continuous in principle but remains exceedingly sharp due to the large parameter ξ_0/a .

The anomalous nature of the topological phase transition is also reflected in the localization properties of the Majorana bound states present in the topological phase [24, 25]. It was first established numerically [24] that the Majorana bound states are no longer exponentially localized in the presence of power-law hopping and pairing. Instead, for $\xi_0 \rightarrow \infty$, the Majorana wavefunction decays as $1/r \ln^2 r$. Interestingly, while not being exponential, this decay is still faster than that of the decay of the hopping and pairing matrix elements. For finite ξ_0 , this power-law decay of the Majorana wavefunction eventually turns into an exponential decay for $r > \xi_0$. These behaviors of the Majorana bound states can be deduced by analyzing the bound-state wavefunctions but are also directly reflected in the splitting of the zero-energy states in a finite chain [24].

The anomalous nature of the topological phase transition becomes apparent when analyzing the localization properties at or near the vertical phase transition lines in figure 3. It turns out that this can actually be done analytically [25]. One finds that for $\xi_0 \rightarrow \infty$, the Majorana end states exhibit an exact *exponential* decay right at the phase transition line. Even more remarkably, this exponential decay is entirely unrelated to the topological gap. Instead, the localization length is on the scale of the lattice spacing of the chain and thus much *smaller* than any scale associated with the topological gap. Physically, the lattice scale emerges because the underlying physics of this exponential localization is Bragg reflection. The vertical phase boundary occurs for $k_h = 2k_F$ (modulo reciprocal lattice vectors of the chain) where the spin helix essentially acts as a perfect Bragg mirror for the zero-energy electrons in the superconductor.

4. Wire limit

4.1. Topological superconductivity

In the previous section, we assumed that the adatom d -levels remain electronically inert. This is no longer adequate when the hopping between the d -levels of adjacent adatoms becomes large. Then, the resulting d -bands cross the Fermi energy of the superconducting substrate. The essential physics becomes transparent in a simplified model of a chain of spin-1/2 Anderson impurities on a superconductor. When a local moment forms for an individual Anderson impurity, the spin-up state is occupied and the spin-down state unoccupied. In general, the energies of the spin-up and spin-down state are asymmetric about the Fermi energy of the substrate. When these states broaden out into bands by hopping between neighboring adatoms, they will cross the substrate Fermi energy at different hopping amplitudes. Consequently, there is a significant parameter range over which only one of the bands crosses the Fermi energy. In this case, the adatom d -levels effectively form a 1D electron system which behaves as a *spin-polarized* wire. This system will generically exhibit topological superconductivity essentially by the same mechanism which underlies previous proposals for topological superconductivity in quantum wires [5, 6].

One specific aspect of the adatom chain in the wire limit is the strong Zeeman splitting of the adatom d -levels. This strong spin polarization implies that spin-orbit coupling of the adatom d -levels is inefficient in inducing p -wave correlations within the d -bands and can be neglected. Indeed, it is well-known that in models with spin-orbit coupling in the wire only, the induced p -wave gap is reduced by the ratio of spin-orbit coupling and spin splitting. However, significant p -wave pairing can still be induced in the adatom d -band when there is significant (Rashba) spin-orbit coupling in the substrate superconductor, as in the half-metal proposals [18, 19].

It is possible to solve a model for a chain of Anderson impurities on a superconducting substrate essentially analytically when treating the on-site interaction U of the Anderson impurities in mean-field approximation [26]. A fully

analytical solution can be worked out in the limit of infinite U when the d bands become fully spin polarized. This solution confirms the formation of a topological phase. It also shows that this topological phase is adiabatically connected to that in the Shiba limit discussed in the previous section.

4.2. Majorana localization

An interesting aspect of the wire limit is that it provides a generic scenario to understand the strong Majorana localization observed in experiment. In general, one expects that the Majorana localization length coincides with the coherence length of the topological superconductor,

$$\xi_M = \frac{\hbar v_F}{\Delta_{\text{top}}}, \quad (14)$$

where v_F denotes the Fermi velocity of the 1D electron system and Δ_{top} the topological gap of the induced superconducting phase. For a strongly dispersing d -band as in the wire limit, we expect that its bare Fermi velocity is of the order of that in typical metals and comparable to the Fermi velocity of the substrate superconductor. Similarly, the topological gap is certainly no larger than the gap of the superconducting substrate. Consequently, we would expect that the Majorana localization length is comparable or larger than the coherence length of the substrate superconductor. In contrast, the experiment observes a localization length which is comparable to the interatomic distance of the adatoms and thus orders of magnitudes smaller than the substrate coherence length.

A possible explanation of this surprising observation was given in [26]. Explicit model calculations in the framework of a chain of Anderson impurities are given in this reference. Here, we emphasize the underlying physical picture. Equation (14) can be made consistent with observation if we interpret v_F as an effective Fermi velocity \tilde{v}_F which is strongly renormalized downward.

In fact, such a renormalization of the Fermi velocity is a feature of the conventional (s -wave) superconducting proximity effect. Consider a 1D (spin-degenerate) wire proximity coupled to a bulk superconducting substrate by hybridization between the wire and the superconducting substrate. An excitation in the wire propagating at subgap energies will virtually enter into the superconductor due to the hybridization between wire and superconducting substrate. Loosely speaking, the relevant time scale on which the excitation leaves the wire is Γ , the decay rate of a quasiparticle in the wire into the substrate in the normal state. The time that the subgap excitation spends in the superconductor is controlled by the characteristic energy scale of the superconductor, namely the gap Δ . As a result, the fraction of time spent by the excitation in the wire is of order Δ/Γ . Thus, if the wire is strongly coupled to the superconductor, $\Gamma \gg \Delta$, the excitation actually spends only a small fraction of time in the wire. It turns out that the excitation effectively propagates along the wire only when it is in the wire. Thus, the Fermi velocity gets renormalized to $\tilde{v}_F \simeq (\Delta/\Gamma)v_F$.

More formally, we can consider the Green function of the wire and account for the coupling to the superconductor

through a self energy [26]. This self energy is strongly energy dependent on the scale Δ . When considering subgap excitations, the self energy is purely real and leads to a renormalization of the quasiparticle weight. For strong hybridization, the quasiparticle weight is strongly suppressed, $Z \simeq \Delta/\Gamma$, reflecting the fact that the excitations have most of their spectral weight in the substrate superconductor. As is familiar from Fermi-liquid theory, a renormalization of the quasiparticle weight implies a corresponding renormalization of the Fermi velocity, $\tilde{v}_F = Zv_F$, in agreement with the intuitive picture sketched above. This calculation also explains why the excitations effectively do not propagate in the superconductor. The excitations can enter the superconductor with different momenta. To leading order, the summation over these momenta makes the self energy independent of the momentum along the wire and thus local in real space.

In [26], we confirm by explicit model calculations that the same physics operates also for the p -wave proximity effect underlying the formation of the topological superconducting phase in the adatom chain in the wire limit. It is interesting to note that this renormalization is quite generic and might also be relevant in other systems realizing Majorana bound states such as semiconductor quantum wires.

In the adatom chain, the hybridization between adatom d -bands and superconducting substrates is governed by atomic energy scales and thus of order 1 eV. This is much larger than the superconducting gap which is of order 10 K. Thus, the mechanism described above leads to a dramatic renormalization of the Fermi velocity. Numerical estimates show that the resulting Majorana localization length can be consistent with the experimental observation.

5. Conclusions

Starting with the seminal suggestion by Fu and Kane that topological superconducting phases with Majorana excitations can be engineered based on conventional superconductors, numerous platforms for Majoranas have been suggested. Among these, hybrid structures of conventional superconductors with 2D topological insulators, semiconductor quantum wires, and chains of magnetic adatoms are most advanced experimentally. Here, we briefly reviewed some theoretical considerations on topological superconductivity and Majoranas in adatom chains. Specifically, we described the system in two regimes which realize different limits of the same topological phase. In the Shiba limit, we assumed that the adatom d -levels are electronically inert and started the Shiba bound states of the individual magnetic adatoms. This leads to a tight-binding model of Shiba bound states which is akin to the familiar Kitaev chain, but qualitatively distinct in that both hopping and pairing in this model are essentially long ranged. We discussed the modifications of the phase diagram and of the Majorana end states which are brought about by this long-range hopping. In the wire limit, the band width of the adatom d -levels becomes large and the d -band crosses the Fermi energy of the substrate superconductor. In this case, the adatom d -bands effectively form a

1D wire. This situation is particularly prone to forming a topological superconducting state when an odd number of the d -levels crosses the Fermi energy. Specifically, we explained how this situation can generically lead to very short Majorana localization lengths as observed in experiment [27].

As emphasized by the experiment [27], chains of magnetic adatoms are a promising direction to search for Majorana excitations. Attractive features of this approach include the variety of physical systems which are available in principle by combining various adatom species with different superconducting substrates, the direct accessibility of the Majorana end states to scanning tunneling microscopy, as well as the ability to manipulate adatoms on an atomic scale by STM. The latter might be useful to realize more elaborate structures which may allow for braiding [40] similar to schemes proposed for some of the other platforms [7]. It will be exciting to probe whether the experiment [27] did indeed observe Majorana excitations, to which degree the experiment is described by minimal models as discussed here, and if so, to explore the Majorana physics in this setting.

Acknowledgments

We thank Ali Yazdani and Andrei Bernevig for discussions, and acknowledge financial support by the Helmholtz Virtual Institute ‘New states of matter and their excitations’, SPP1285 and SPP 1666 of the Deutsche Forschungsgemeinschaft, the Studienstiftung d.dt.Volkes, and NSF DMR Grants 0906498 and 1206612. We are grateful to the Aspen Center for Physics, supported by NSF Grant No. PHYS-106629, for hospitality while this line of research was initiated.

References

- [1] Alicea J 2012 *Rep. Prog. Phys.* **75** 076501
- [2] Beenakker C W J 2013 *Annu. Rev. Condens. Matter Phys.* **4** 113
- [3] Fu L and Kane C L 2008 *Phys. Rev. Lett.* **100** 096407
- [4] Fu L and Kane C L 2009 *Phys. Rev. B* **79** 161408(R)
- [5] Lutchyn R M, Sau J D and Sarma S D 2010 *Phys. Rev. Lett.* **105** 077001
- [6] Oreg Y, Refael G and von Oppen F 2010 *Phys. Rev. Lett.* **105** 177002
- [7] Alicea J, Oreg Y, Refael G, von Oppen F and Fisher M P A 2011 *Nat. Phys.* **7** 412
- [8] Mourik V, Zuo K, Frolov S M, Plissard S R, Bakkers E P A M and Kouwenhoven L P 2012 *Science* **336** 1003
- [9] Das A, Ronen Y, Most Y, Oreg Y, Heiblum M and Shtrikman H 2012 *Nat. Phys.* **8** 887
- [10] Churchill H O H, Fatemi V, Grove-Rasmussen K, Deng M T, Caroff P, Xu H Q and Marcus C M 2013 *Phys. Rev. B* **87** 241401(R)
- [11] Rokhinson L P, Liu X and Furdyna J K 2012 *Nat. Phys.* **8** 795
- [12] Deng M T, Yu C L, Huang G Y, Larsson M, Caroff P and Xu H Q 2012 *Nano Lett.* **12** 6414
- [13] Finck A D K, van Harlingen D J, Mohseni P K, Jung K and Li X 2013 *Phys. Rev. Lett.* **110** 126406

- [14] Hart S, Ren H, Wagner T, Leubner P, Mühlbauer M, Brüne C, Buhmann H, Molenkamp L W and Yacoby A 2014 *Nat. Phys.* **10** 638
- [15] Pribiag V S, Beukman A J A, Qu F, Cassidy M C, Charpentier C, Wegscheider W and Kouwenhoven L P 2015 *Nat. Nanotechnol.* doi:10.1038/nnano.2015.86
- [16] Kitaev A Y 2001 *Phys. Usp.* **44** 131
- [17] Kitaev A 2003 *Ann. Phys.* **303** 2
- [18] Duckheim M and Brouwer P W 2011 *Phys. Rev. B* **83** 054513
- [19] Chung S B, Zhang H J, Qi X L and Zhang S C 2011 *Phys. Rev. B* **84** 060510(R)
- [20] Nadj-Perge S, Drozdov I K, Bernevig B A and Yazdani A 2013 *Phys. Rev. B* **88** 020407(R)
- [21] Choy T-P, Edge J M, Akhmerov A R and Beenakker C W J 2011 *Phys. Rev. B* **84** 195442
- [22] Kjaergaard M, Wölms K and Flensberg K 2012 *Phys. Rev. B* **85** 020503
- [23] Martin I and Morpurgo A 2012 *Phys. Rev. B* **85** 144505
- [24] Pientka F, Glazman L I and von Oppen F 2013 *Phys. Rev. B* **88** 155420
- [25] Pientka F, Glazman L I and von Oppen F 2014 *Phys. Rev. B* **89** 180505(R)
- [26] Peng Y, Pientka F, Glazman L I and von Oppen F 2015 *Phys. Rev. Lett.* **114** 106801
- [27] Nadj-Perge S, Drozdov I K, Li J, Chen H, Jeon S, Seo J, MacDonald A H, Bernevig B A and Yazdani A 2014 *Science* **346** 602–7
- [28] Yu L 1965 *Acta Phys. Sin.* **21** 75
- [29] Shiba H 1968 *Prog. Theor. Phys.* **40** 435
- [30] Rusinov A I 1968 *Zh. Eksp. Teor. Fiz. Pisma Red.* **9** 146
Rusinov A I 1969 *JETP Lett.* **9** 85
- [31] Balatsky A V, Vekhter I and Zhu J-X 2006 *Rev. Mod. Phys.* **78** 373
- [32] Abrikosov A A 1988 *Fundamentals of the Theory of Metals* (Amsterdam: North-Holland)
- [33] Klinovaja J, Stano P, Yazdani A and Loss D 2013 *Phys. Rev. Lett.* **111** 186805
- [34] Braunecker B and Simon P 2013 *Phys. Rev. Lett.* **111** 147202
- [35] Vazifeh M M and Franz M 2013 *Phys. Rev. Lett.* **111** 206802
- [36] Brydon P M R, Hui H-Y and Sau J D 2014 arXiv: 1407.6345
- [37] Braunecker B, Japaridze G I, Klinovaja J and Loss D 2010 *Phys. Rev. B* **82** 045127
- [38] Menzel M, Mokrousov Y, Wieser R, Bickel J E, Vedmedenko E, Blügel S, Heinze S, von Bergmann K, Kubetzka A and Wiesendanger R 2012 *Phys. Rev. Lett.* **108** 197204
- [39] Kim Y, Cheng M, Bauer B, Lutchyn R M and Sarma S D 2014 *Phys. Rev. B* **90** 060401(R)
- [40] Li J, Neupert T, Bernevig B A and Yazdani A 2014 arXiv:1404.4058